Int J. Heat Mass Transfer. Vol. 23, pp. 547–557
© Pergamon Press Ltd. 1980. Printed in Great Britain

0017-9310/80/0401-0547 $02.00/0

DRY PATCH FORMATION IN LIQUID FILMS FLOWING IN A HEATED HORIZONTAL CHANNEL

ARIEL SHARON* and ALUF ORELL
Department of Chemical Engineering, Technion-Israel Institute of Technology, Haifa, Israel

(*Received* 21 *November* 1978 *and in revised form* 3 *July* 1979)

Abstract — The hydrodynamic and heat-transfer characteristics of thin liquid films flowing in a horizontal heated channel were investigated experimentally and analytically for the purpose of modelling film breakdown and dry patch formation. A physical criterion for film breakdown was formulated and incorporated in a model, containing one empirical parameter, that successfully predicts the critical heat flux for water and organic liquids for $5 < Re < 100$. Equations for predicting axial film thickness profiles for both heated and unheated film flow were derived based on a proposed downstream boundary condition.

NOMENCLATURE

A, a, coefficients;
B, coefficient, equation (A1);
b, coefficient, defined by equation (27);
C, coefficient, equation (22);
C_i, parameter, defined by equation (17);
E, specific energy;
Fr, Froude number, defined by equation (36);
g, gravitational acceleration;
H, local film thickness;
H_c^*, critical film thickness at $x = L_H$;
H_L, film thickness at channel outlet;
h, heat-transfer coefficient;
k, thermal conductivity;
L, channel total length;
L_H, combined length of the entrance and heated sections;
l, coefficient;
Ma, Marangoni number, defined by equation (34);
m, parameter, defined by equation (33);
Nu_x, local Nusselt number, $Nu_x = \dfrac{hx}{k}$;
P, pressure;
Pr, Prandtl number;
Q, volumetric flow rate per unit width;
Q^*, volumetric flow rate;
q, heat-transfer rate;
R, film surface radius of curvature;
Re, Reynolds number, defined by equation (36);
Re_x, local Reynolds number, $Re_x = \dfrac{\rho \bar{u} x}{\mu}$;
T, temperature;
T_s, film surface temperature;
T_w, heating surface temperature;
u, velocity in x direction;
$\bar{u}$, average velocity in x direction;
v, velocity in y direction;
x, axial distance from channel inlet;
y, vertical distance from channel bottom.

Greek letters

α, thermal diffusivity;
γ, surface tension temperature gradient, $\left|\mathrm{d}\sigma/\mathrm{d}T\right|$;
μ, viscosity;
ν, kinematic viscosity;
ρ, density;
σ, surface tension.

Subscripts

at, atmospheric;
c, critical;
E, energy;
M, momentum.

INTRODUCTION

FLOWING thin liquid films in contact with a solid wall are often used to cool heated surfaces and in other applications that involve heat or mass transfer. When the applied heat flux or concentration driving force exceeds a critical value the film breaks down and forms dry patches. The exposure of the solid surface in any installation that employs continuous flowing films can reduce its effectiveness and is therefore undesirable.

Previous work has centered mainly on the disruption of wavy falling films due to heating [1–4] although the phenomenon can also occur in film flow over a heated horizontal surface [5]. These studies indicate that film breakdown is induced by thermocapillary forces that develop as the heated film flows over vertical or horizontal surfaces. Attention has also been focused on the related problems of the stability of heated falling films [6–9] and of dry patches formed on heated walls [10, 11].

While the mechanism of the disruption of heated falling films is fairly well understood the problem of

*Present address: Department of Chemical Engineering, Northwestern University, Evanston, Illinois, U.S.A.

predicting the critical heat flux–flow rate relationship at which the film breaks down has not yet been solved satisfactorily. Furthermore, a reliable criterion for film rupture at the critical heat flux is still lacking.

Dry patch formation on vertical surfaces is complicated by the presence of waves. This effect was eliminated in the present study by considering the case of film breakdown in a horizontal channel geometry where the laminar film surface remains smooth up to Reynolds number of about 300.

The aims of this experimental and theoretical investigation were threefold. First, to seek a detailed mechanism of film breakdown of smooth, non-wavy horizontal flow. Second, to propose and formulate a physical criterion for film rupture. Third, to develop a mathematical model for predicting the critical heat flux.

Elucidation of the film breakdown mechanism requires first that the effect of heat transfer on film flow be adequately understood. Consequently, this study is concerned with three interrelated problems:

1. Isothermal horizontal film flow.
2. The hydrodynamics and heat-transfer characteristics of flowing films heated from below.
3. Film breakdown and dry patch formation.

EXPERIMENTAL

Film flow experiments were conducted under both isothermal and constant heat flux conditions in a horizontal channel shown in Fig. 1. The 11 cm wide channel was made of Pertenex, a thermal insulating plastic. The effective film flow length was 32 cm and consisted of 3 zones: an unheated entrance section 8 cm long, a heated section 15 cm long and a post-heated section. The liquid discharged from the channel through an inclined Pertenex spillway.

The heating section spanned the entire channel width and consisted of an electrically heated copper plate mounted flush with the channel bottom. The entire Pertenex–copper surface was ground flat to a tolerance of $\pm$ 0.0025 cm. The channel was mounted on a supporting frame equipped with levelling screws.

Distilled water was used as the main test liquid. In several experiments a 9 m mole/l solution of Triton-X-100 surfactant was used to determine the effect of surface tension on the characteristics of heated and unheated films.

The film thickness was measured to within 5×10^{-3} mm by means of a micrometer needle probe that was mounted on a traversing mechanism. The position of the liquid surface was determined electrically by forming a circuit between the probe and the channel copper base plate that consisted of a 6 V DC source and a high sensitivity galvanometer in series. Contact between the needle tip and the liquid was indicated by a sharp deflection of the galvanometer. The results of this method compared very favorably with visual observations of the probe contact.

The vertical temperature profile within the heated film and its surface temperature were measured by a BLH copper–constantan microthermocouple mounted on a micrometer. The thermocouple wires, each of 0.0025 cm in diameter, were housed in a stainless steel sheath of 0.035 cm O.D. The thermocouple, no doubt, introduced some distortion to the flow and temperature fields. However, due to its small size the effect was considered to be minimal in this case. The thermocouple error due to fin effect [22] were calculated and found to be negligibly small since its maximum immersion depth in the flowing film was 0.13 cm, hence practically the entire sheath length was exposed to the atmosphere. No additional corrections were applied to the thermocouple readings. The temperature measurement accuracy was within $\pm$ 1°C.

The heated film experiments were performed under quasi-steady state condition by increasing the power level at a given flow rate in a stepwise manner. After each power change and prior to taking any measurement, the system was given ample time to reach steady state, as indicated by the heating section thermocouples. Smaller power steps were used upon approaching the critical heat flux at which the film ruptured, forming a dry patch.

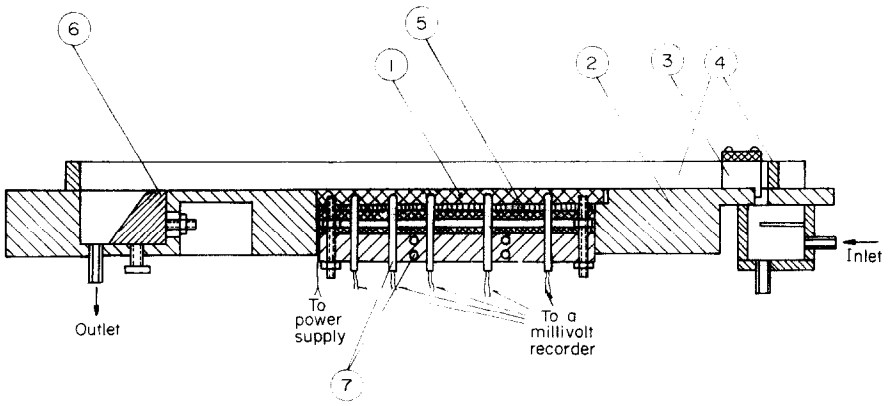

FIG. 1. Experimental apparatus. (1) Heated copper plate. (2) Channel base plate. (3) Flow guiding vanes. (4) Channel side walls. (5) Heating element. (6) Spillway. (7) Thermocouples.

ISOTHERMAL HORIZONTAL FILM FLOW

Isothermal laminar film flow in near-horizontal and horizontal channels has been investigated previously both experimentally and theoretically [12–16]. Yet, the case of horizontal flow of thin films and, in particular, the flow characteristics at the channel outlet deserve further considerations. In this section we derive an analytical expression for predicting the axial film thickness profile in a horizontal channel based on the liquid discharge mechanism at the channel exit.

The local film thickness in a horizontal channel flow is governed by the following differential equation:

$$\frac{dH}{dx} = \frac{3Qv}{\frac{6}{5}Q^2 - gH^3} \tag{1}$$

where Q is the volumetric flow rate per unit channel width. Equation (1) can be derived by integrating the equations of motion [13] or by an integral momentum balance [12] assuming a semi-parabolic velocity profile. Upon neglecting the inertial terms of the Navier–Stokes equations equation (1) reduces to [15]:

$$\frac{dH}{dx} = -\frac{3Qv}{gH^3}. \tag{2}$$

The integration of equation (1) or (2) for a channel of finite length, L, requires an appropriate boundary condition. Since in open mild-slope channel flow the channel outlet controls the upstream film thickness [17, 18] a natural choice is the film thickness at the channel exit, where $x = L$.

A variety of boundary conditions at the channel outlet have been proposed in the past based on theoretical [13, 19] and empirical [12, 15, 16] considerations. None of these was found to be adequate in this investigation.

Before formulating an appropriate physical boundary condition it is instructive first to analyse equation (1) for the purpose of defining the possible modes of flow in the channel.

The first term in the denominator of the RHS of equation (1) represents the inertial force whereas the second term accounts for the gravity force. Equating the denominator to zero results in a critical film thickness

$$H_{c,M} = \left(\frac{6Q^2}{5g}\right)^{1/3} \tag{3}$$

which is characterized by an infinite film thickness gradient, namely $(dH/dx) \to \infty$. Such a condition defines the critical flow mode which usually occurs at the channel outlet. In the case where $H > H_{c,M}$ the film thickness decreases in the downstream direction and the flow is termed subcritical. This is the normal mode of horizontal film flow since $H_{c,M}$ is quite small for laminar flow. If $H < H_{c,M}$ the film thickness increases in the flow direction and the flow is supercritical. Such a mode is characteristic of hydraulic jump [17]. It is worthwhile noting that the expression for $H_{c,M}$ was derived from the momentum equation.

In dealing with open channel flow it is commonly accepted that the liquid attains a minimum energy at the channel exit cross-section [17, 18]. Consequently, the required boundary condition may be derived on the basis of minimum energy considerations.

If the film specific energy is taken as the sum of its kinetic and potential energy, then its minimization with respect to the local film thickness, H, yields a film thickness which is identical to $H_{c,M}$ given by equation (3). Gollan and Sideman[13] suggested that the minimum-energy film thickness be used as a boundary condition at the downstream edge of near-horizontal channels. However, film thickness data of this investigation and others[14, 16] for thin films have indicated that $H_{c,M}$ is much smaller than the experimental values at the horizontal channel outlet and that surface tension has a noticeable effect on the film thickness at this cross-section. Indeed, large film curvatures were observed at the downstream edge of the channel. Consequently, the film surface energy is an important component of the total film energy at the outlet section and should not be neglected in horizontal flow of thin films.

Consequently, the total specific energy of the film at the channel exit, expressed as energy head, is thus:

$$E = H + \frac{3Q^2}{5gH^2} + \frac{\sigma}{\rho g}\cdot\frac{1}{R}. \tag{4}$$

The first term on the RHS is the potential specific energy, the second term represents the average kinetic specific energy

$$\left(\frac{1}{H}\int_0^H \frac{u^2}{2g}\,dy\right)$$

and the last term is the specific surface energy. R is the film surface radius of curvature measured through the liquid.

The free surface curvature in the axial direction may be adequately approximated by

$$\frac{1}{R} = -\frac{d^2H}{dx^2} \tag{5}$$

that in conjunction with equation (2) yields:

$$\frac{1}{R} = \frac{27Q^2v^2}{g^2H^7}. \tag{6}$$

Combining equations (4) and (6) and setting dE/dH at the channel outlet to be zero results in

$$1 - \frac{6Q^2}{5g}H_{c,E}^{-3} - \frac{189\sigma Q^2v^2}{\rho g^2}H_{c,E}^{-8} = 0 \tag{7}$$

where $H_{c,E}$ is the critical film thickness based on energy considerations. Although $H_{c,E}$ is given implicitly it can easily be solved for numerically.

Equation (1) can now be integrated using the boundary condition

$$H = H_{c,E} = H_L \quad \text{at } x = L \tag{8}$$

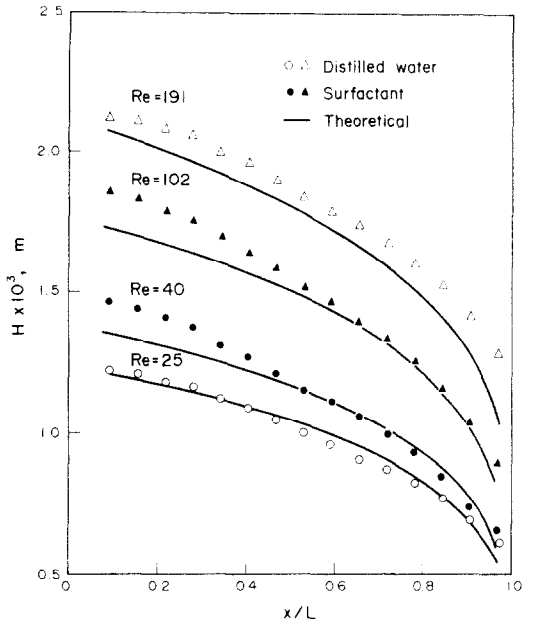

FIG. 2. Isothermal film thickness profiles. Distilled water and surfactant solution.

to yield:

$$\frac{g}{4}(H^4 - H_L^4) - \frac{6Q^2}{5}(H - H_L) = 3Qv(L - x). \quad (9)$$

Equation (9) in conjunction with (7) was used to predict the axial film thickness profile for laminar horizontal channel flow.

The predicted film thickness profile was compared with experimental data for distilled water, a surfactant solution and a variety of organic liquids [16] over the range $10 \leq Re \leq 300$. Typical results are shown in Figs. 2 and 3. The agreement between the predicted and observed values is very good for $Re < 150$ and the average deviation is less than $\pm 5\%$. Equation (9) underpredicts the film thickness for $Re > 150$ but the deviations do not exceed 10%.

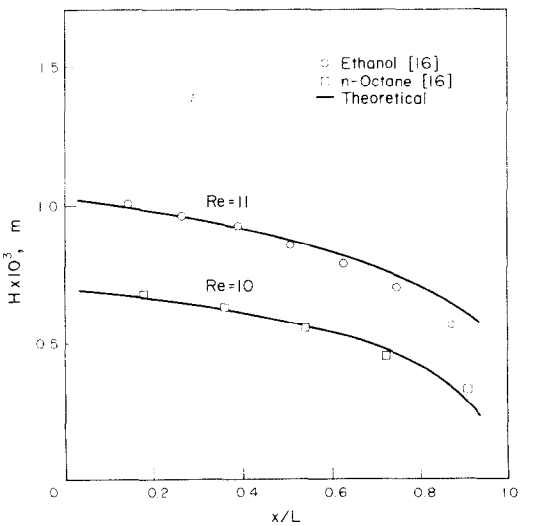

FIG. 3. Isothermal film thickness profiles. Organic liquids.

FILM FLOW IN A HEATED HORIZONTAL CHANNEL

This section deals with the effect of heat transfer on the axial film thickness profile. Consider the case where a thin liquid film is flowing in laminar steady flow over a horizontal channel that is heated uniformly. The governing equations are as follows:

Continuity:

$$\int_0^H u\,dy = \bar{u}H = Q. \quad (10)$$

Momentum, in the axial direction:

$$u\frac{\partial u}{\partial x} + v\frac{\partial u}{\partial y} = -\frac{1}{\rho}\frac{\partial P}{\partial x} + \nu\frac{\partial^2 u}{\partial y^2}. \quad (11)$$

Momentum, in the vertical direction:

$$\frac{\partial P}{\partial y} = -\rho g \quad (12)$$

where y is a vertical coordinate measured from the bottom of the channel.

The boundary conditions are:

$$u = v = 0 \quad \text{at } y = 0 \quad (13)$$

$$\mu\frac{\partial u}{\partial y} = \frac{d\sigma}{dx} = \frac{d\sigma}{dT}\cdot\frac{dT_s}{dx} \quad \text{at } y = H. \quad (14)$$

Equation (14) equates the viscous shear stress with the tangential component of the thermocapillary force.

In addition, the capillary pressure at the curved liquid surface is given by:

$$P_s - P_{at} = \frac{\sigma}{R} = -\sigma\frac{d^2H}{dx^2} \quad \text{at } y = H. \quad (15)$$

The solution of equations (10)–(12) is given in the Appendix. The resulting differential equation for the film thickness profile is:

$$\frac{dH}{dx} = \frac{3Qv + \frac{3}{2}C_i\nu H^2}{\frac{6}{5}Q^2 + \frac{C_iQ}{20}H^2 - gH^3 + \frac{C_i^2}{40}H^4} \quad (16)$$

where C_i is defined as

$$C_i = \frac{\gamma}{\mu}\cdot\frac{dT_s}{dx} \quad (17)$$

and γ is the absolute value of the surface tension temperature gradient.

A simplified version of equation (16) may be obtained by neglecting the inertial terms in equation (11), namely:

$$\frac{dH}{dx} = -\frac{3Qv + \frac{3}{2}C_i\nu H^2}{gH^3} \quad (18)$$

It is interesting to note that equation (18) is identical to the one derived by Yih [20] for the case of the flow of a horizontal thin liquid film that is induced by longitu-

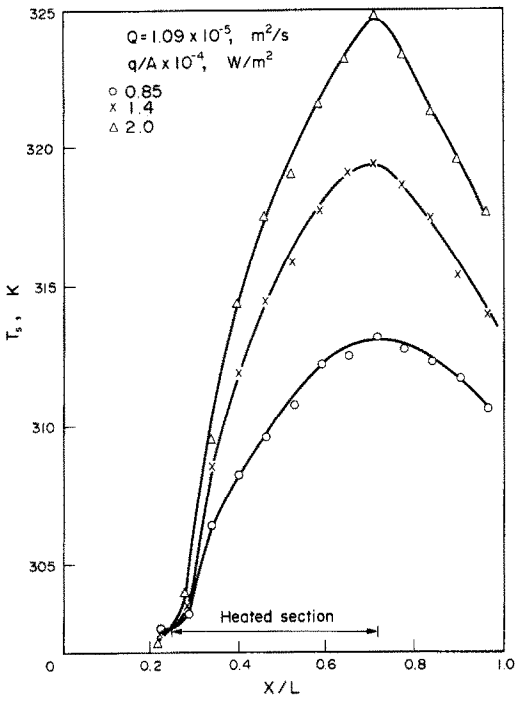

FIG. 4. Experimental film surface temperature profiles.

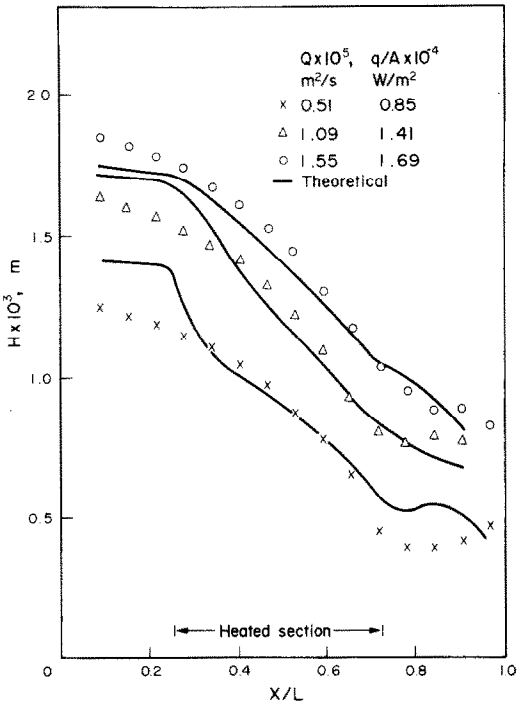

FIG. 5. Heated film thickness profiles.

dinal variation of surface tension.

Equation (16) can be solved for the heated film thickness profile provided that the film surface temperature is known. Theoretical evaluation of the surface temperature profile of a heated horizontal film with variable thickness is by no means a simple problem as can be judged from the analysis of a simpler case of a heated falling film in laminar flow [21]. This difficulty was circumvented in the present investigation by evaluating the film surface temperature experimentally. Consequently, equation (16) can be applied to the three zones of the experimental channel: (1) the unheated entrance section, where the film is isothermal; (2) the heated section, where the surface temperature increases in the downstream direction; (3) the post-heated section, where the surface temperature decreases due to heat losses to the surrounding.

Equation (16) was solved numerically over the entire channel length using the experimental surface temperature data and the downstream boundary condition, equations (7) and (8). Some typical surface temperature profiles are shown in Fig. 4. Predicted film thickness profiles over the entire channel are compared with measured profiles in Fig. 5. Considering the difficulty in evaluating the axial surface temperature gradient the agreement over the heated section is quite good. Deviations occur mainly at both ends of the channel but do not exceed $\pm$ 15%.

In as much as equation (16) applies to non-evaporating films the extent of the evaporation of water films in the heated channel was checked by measuring the flow rates at the channel inlet and outlet at the highest heat flux, i.e. the critical heat flux. Evaporation losses, defined as the relative decrease of the inlet flow rate, ranged from 0.5 to 6.3% indicating that their effect on the film thickness was small enough to be neglected.

FILM BREAKDOWN AND DRY PATCH FORMATION

Heating has a marked effect on the film thickness profile relative to isothermal flow, as can be judged from Fig. 6. At a given flow rate the heated film becomes thicker in the upstream section and thins down rapidly as it approaches the downstream edge of the heating surface. The phenomenon becomes more pronounced as the heat flux is increased. Eventually, when the heat flux attains a critical value the film

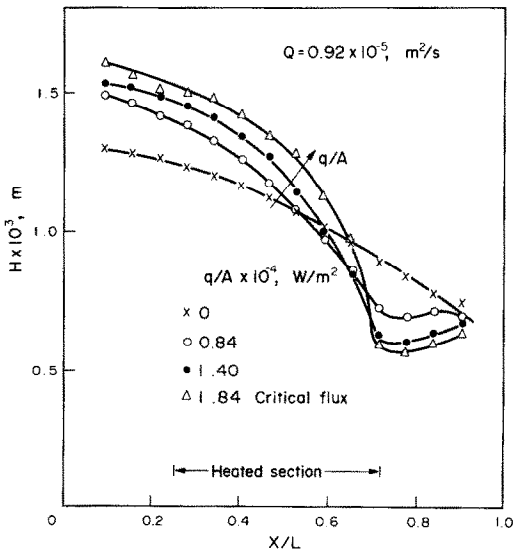

FIG. 6. Effect of applied heat flux on film thickness profile.

ruptures. Thus, heated horizontal films are characterized by larger film thickness gradients and exhibit a concave interface near the exit from the heating section.

In this section some visual observations pertaining to film breakdown will be presented, a film rupture mechanism will be proposed, a criterion for film breakdown will be formulated and a model for predicting the critical heat flux will be presented.

VISUAL OBSERVATIONS

At near-critical heat fluxes, but prior to film breakdown, some strong disturbances appear on the film surface near the outlet of the heated section. Consequently, the locally thinned film becomes unstable and any slight disturbance will cause its breakdown. Thus, either a "premature" or "delayed" breakdown can occur depending upon the extent of small uncontrollable disturbances. The critical heat flux at which a spontaneous breakdown occurs is thus hard to reproduce and deviations up to $\pm 10\%$ from an average value may be expected.

Film rupture and dry patch formation always occur at the downstream edge of the heated section. The first patch appears usually near one of the channel side walls followed by additional patches that form at random locations along the edge. The patches are relatively small, maintain a constant size and are confined to the heating surface only. As the heat flux is increased beyond the critical value the patches grow in size and extend into the post-heated section.

FILM BREAKDOWN MECHANISM

For the purpose of analyzing the conditions leading to film rupture it is instructive to consider the forces acting on the liquid film as it flows over the heating surface. These forces include: inertial, gravitational and surface forces. The surface force consists of two components: one due to axial variation of surface tension, or thermocapillary shear stress, and one due to local changes of film curvature that result in capillary pressure force acting along the film surface.

Inertial and gravitational forces tend to stabilize the film while thermocapillary shear may lead to film instability. In addition, if large curvature changes occur in the longitudinal direction the effect of capillary pressure difference can become important and might enhance the instability. The proposed mechanism for film breakdown due to surface forces is illustrated schematically in Fig. 7.

The critical region that affects the film instability is the downstream edge of the heated section. As the heated film flows past this cross-section it begins to cool off, as indicated by Fig. 4. The reversal of the surface temperature gradient directly affects the thermocapillary force direction and hence the film surface curvature.

Over the heated section, where the surface temperature gradient is positive, the thermocapillary force opposes the flow. Consequently, the film accelerates more rapidly relative to the isothermal flow case and the film thickness gradient increases. This effect becomes more pronounced near the outlet of heated section as manifested by the steep thickness gradient, as shown in Fig. 6.

This situation reverses in the post-heated section. Here the thermocapillary force acts along the flow direction, the film decelerates and its thickness increases. The marked change in film curvature that occurs near the critical cross-section results in capil-

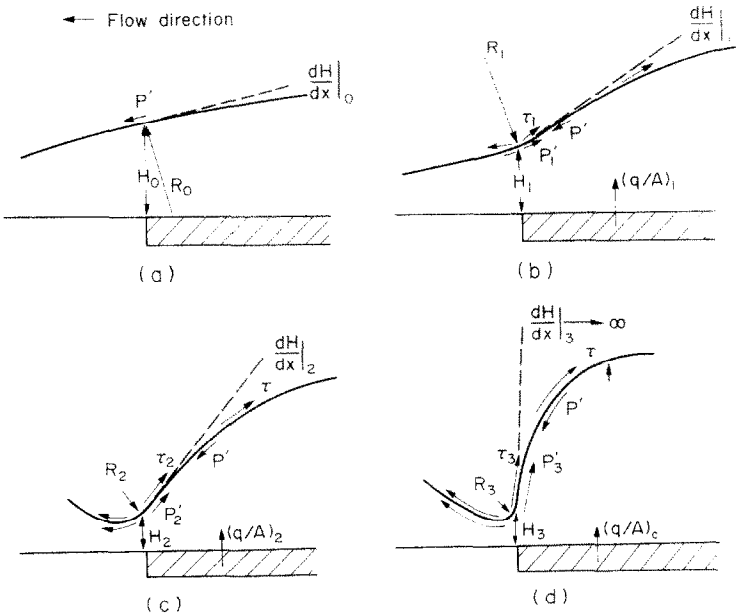

FIG. 7. Effect of surface forces on film curvature at the downstream edge of the heated section. (a) Isothermal flow. (b) Low heat flux. (c) Intermediate heat flux. (d) Near-critical heat flux.

lary pressure forces that contribute further to the film instability, as indicated schematically in Fig. 7, by the P' arrows.

Upon increasing the heat flux level the temperature gradient becomes steeper and the minimum film thickness decreases. Consequently, the effect of the perturbing surface forces becomes more pronounced. Eventually, any small disturbance of the film will be amplified thus causing its breakdown.

FILM BREAKDOWN CRITERION

A rigorous formulation of a physical criterion for film breakdown is by no means an easy task. Stability analysis of flowing heated films, by its very nature, cannot yield a viable criterion for actual film rupture. Furthermore, the existing stability analyses of a heated falling film [6, 7, 9] are inapplicable to horizontal film flow. Consequently, a different approach was taken in order to establish a physical criterion that can readily be used to predict the critical heat flux.

Consider the shape of the heated film in the neighborhood of the downstream edge of the heated section at near-critical heat flux. The flow over the heated section has the features of a subcritical flow, namely, the film thickness decreases in the flow direction. On the other hand, the flow in the post-heated section is supercritical in nature and the film thickens. Consequently, critical flow conditions must prevail at the cross section of the downstream edge of the heated section. As the critical film thickness is quite small and since critical flow is known to be unstable any small disturbance will lead to film rupture.

The critical film thickness, H_c^*, is a necessary but not sufficient condition for film breakdown. Experimental data indicate that the film may attain a minimum thickness at heat fluxes that are somewhat lower than the critical value. However, as the critical heat flux is approached the film thickness gradient near the downstream cross section becomes very large and may be considered as tending to infinity.

On the basis of these considerations the film breakdown criterion is formulated as follows:

$$\text{as} \quad q/A \to (q/A)_c$$

$$\text{and} \quad \left.\begin{aligned} H &\to H_c^* \\ \frac{dH}{dx} &\to \infty \end{aligned}\right\} \text{at } x = L_H \tag{19}$$

where L_H is the axial distance to the downstream edge of the heated section.

PREDICTION OF CRITICAL HEAT FLUX

The proposed model for predicting the critical heat flux is based on the thickness profile of the heated film, the breakdown criterion and an appropriate relationship between the film surface temperature, applied heat flux and flow rate.

Equation (18) was found to be quite adequate for evaluating the film profile over the heated section. Consequently, the expression for the critical film thickness at $x = L_H$ is obtained upon rearranging equation (18),

$$-\frac{dH}{dx}\left(\frac{gH^3}{3\nu}+\frac{\gamma H^2}{2\mu}\cdot\frac{dT_s}{dx}\cdot\frac{1}{dH/dx}\right)=Q \tag{20}$$

and applying the breakdown criterion, equation (19). The result is

$$H_c^* = -\frac{3}{2}\frac{\gamma}{\rho g}\lim_{H'\to\infty}\left(\frac{T_s'}{H'}\right) \tag{21}$$

where the prime denotes a derivative with respect to x. The evaluation of H_c^* requires that the film surface temperature be known.

To avoid the difficult problem of solving the momentum and energy equations simultaneously for the axial surface temperature profile of a heated film we resort to a semi-empirical approach that relates T_s to the applied heat flux. The vertical temperature profile inside the flowing film was measured over a wide range of flow rates, heat fluxes and axial positions along the heating section. Typical profiles are shown in Fig. 8. The extensive data indicate that the film temperature is a linear function of the vertical position y:

$$T(x, y) = T_w(x) - C(x)y \tag{22}$$

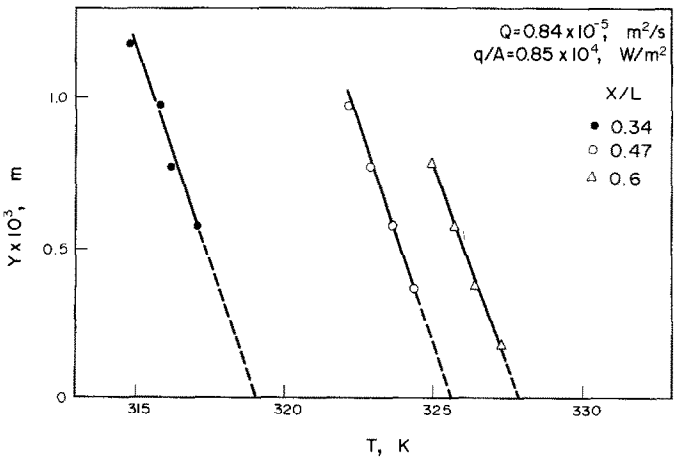

FIG. 8. Vertical temperature profiles within the heated film.

where $T_w(x)$ is the extrapolated film temperature at $y = 0$ and $C(x)$ is a parameter yet to be determined.

We relate $C(x)$ to the flow and heat-transfer conditions by defining a film heat-transfer coefficient thus

$$h(x) = \frac{qA}{T_w(x) - T_s(x)}. \tag{23}$$

Consequently,

$$C(x) = \frac{qA}{h(x)H(x)}. \tag{24}$$

By analogy to convective heat transfer in a thermal boundary layer for laminar flow over a horizontal heated plate the film heat-transfer coefficient is correlated by

$$Nu_x = a\,Re_x^{1/2} = a\left(\frac{Qx}{\nu H(x)}\right)^{1/2} \tag{25}$$

where the Prandtl number has been incorporated into the coefficient a. Consequently,

$$C(x) = \frac{qA}{b}\left(\frac{x}{QH(x)}\right)^{1/2} \tag{26}$$

where

$$b = ak/\nu^{1/2}. \tag{27}$$

The film surface temperature is obtained by combining equations (22) and (26) at $y = H$

$$T_s = T_w(x) - \frac{q/A}{b}\left(\frac{xH(x)}{Q}\right)^{1/2}. \tag{28}$$

To evaluate the limit in equation (21) we obtain the ratio T_s'/H' from equation (28) as follows:

$$\frac{T_s'}{H'} = \frac{T_w'(x)}{H'} - \frac{q/A}{2bQ^{1/2}}\left[\frac{1}{H'}\left(\frac{H}{x}\right)^{1/2} + \left(\frac{x}{H}\right)^{1/2}\right]. \tag{29}$$

Hence, at the critical heat flux, $(q/A)_c$:

$$\lim_{\substack{H'\to\infty \\ x=L_H}}\left(\frac{T_s'}{H'}\right) = -\frac{(q/A)_c}{2b}\left(\frac{L_H}{H_c^* Q}\right)^{1/2} = -\tfrac{1}{2}(C_{x=L_H})_c \tag{30}$$

assuming that T_w' is finite. Combining equations (21) and (30) and solving for the critical heat flux:

$$\left(\frac{q}{A}\right)_c = \frac{4}{3}\frac{\rho g b}{\gamma}\left(\frac{H_c^{*3} Q}{L_H}\right)^{1/2}. \tag{31}$$

We assume that at a given flow rate the critical film thickness for film rupture at the downstream edge of the heating section and the unheated film thickness at the channel exit, equation (7), are linearly dependent, i.e. $H_c^* = lH_L$; hence

$$\left(\frac{q}{A}\right)_c = \frac{4\rho g m}{3\gamma}(H_L^3 Q)^{1/2} \tag{32}$$

where

$$m = b\left(\frac{l^3}{L_H}\right)^{1/2}. \tag{33}$$

Table 1. Values of m for various liquids and channels

Source	Test Liquid	m $\left(\frac{W \cdot s^{1/2}}{m^{5/2} \cdot K}\right) \times 10^{-3}$
This work	Distilled water	13.88
Ydidsion [16]	Ethanol	3.61
	n-Dodecane	2.05
	n-Hexane	2.08
	Cyclohexane	2.75
	n-Octane	4.17

The coefficient m depends upon the liquid properties (through coefficient b), the geometry of the heated channel and the coefficients l and b, which at present are not readily determined. Consequently, m was treated as an empirical coefficient and evaluated for each test liquid by equation (32) using the available critical heat flux data. Numerical values of m for distilled water obtained in this investigation and for organic liquids, based on data of Ydidsion [16], are given in Table 1.

The predicted relationship between the critical heat flux and flow rate is compared with the experimental data for distilled water and organic liquids in Figs. 9 and 10. The agreement between the predicted and observed values is very good in view of the fact that the critical heat flux is not a single-value variable. The deviation does not exceed $\pm$ 10% and is within the limit of the experimental error.

It is advantageous to render equation (31) dimensionless by using the Marangoni number, defined as

$$Ma = \frac{H(T_w - T_s)}{\alpha\mu}\left|\frac{d\sigma}{dT}\right| = \frac{C(x)\gamma H^2}{\alpha\mu}. \tag{34}$$

The critical Marangoni number for film rupture is evaluated in terms of the pertinent variables by combining equations (21), (30) and (34):

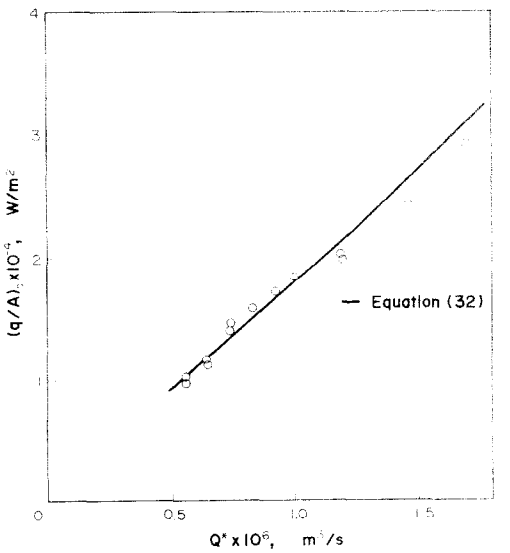

FIG. 9. Critical heat flux vs flow rate. Distilled water.

$$Ma_c = \frac{\gamma(q/A)_c}{b\alpha\mu}\left(\frac{L_H H_c^{*3}}{Q}\right)^{1/2}. \quad (35)$$

Defining the following dimensionless numbers:

$$Re = \frac{4Q}{\nu}\,;\; Fr = \frac{\bar{u}}{\sqrt{gH}}\,;\; Pr = \frac{\nu}{\alpha} \quad (36)$$

and substituting for $(q/A)_c$ from equation (31) there results:

$$(Ma \cdot Fr^2)_c = \frac{1}{12} Re^2\, Pr. \quad (37)$$

Equation (37) relates the critical flow and heat-transfer conditions at the downstream edge of the heating section to the film flow rate. The critical Froude number characterizes the critical flow that occurs at the cross-sectional plane at $x = L_H$, where $H = H_c^*$, and Ma_c characterizes the temperature gradient across the film at this plane, namely $\Delta T/H_c^*$.

Equation (37) is semi-empirical in that it contains one empirical coefficient, m, which appears in the LHS:

$$(Ma \cdot Fr^2)_c = \frac{\gamma(q/A)_c}{\alpha\mu g m}\left(\frac{Q}{H_L}\right)^{3/2}. \quad (38)$$

A comparison of the predicted $(Ma \cdot Fr^2)_c$ values, namely the RHS of equation (37), with the experimental values computed from equation (38) is presented in Fig. 11. The required physical and thermal properties of water were evaluated at 50°C, a representative average of the observed cross-sectional mean film temperatures. The properties of the organic liquids were taken at 25°C since film temperature data were unavailable. As can be seen equation (37) correlates

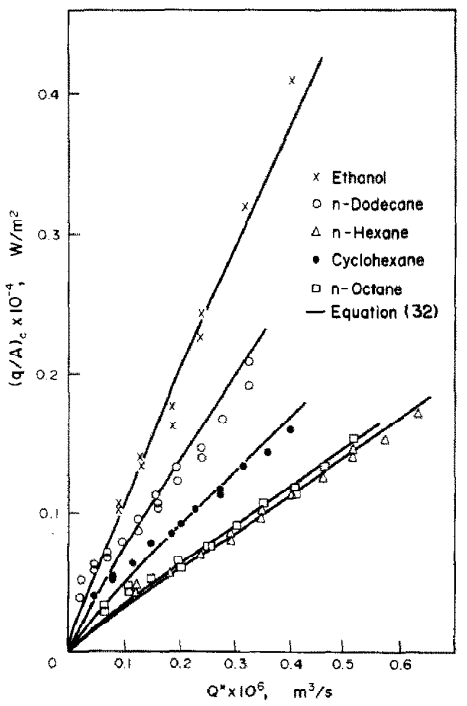

FIG. 10. Critical heat flux vs flow rate. Organic liquids [16].

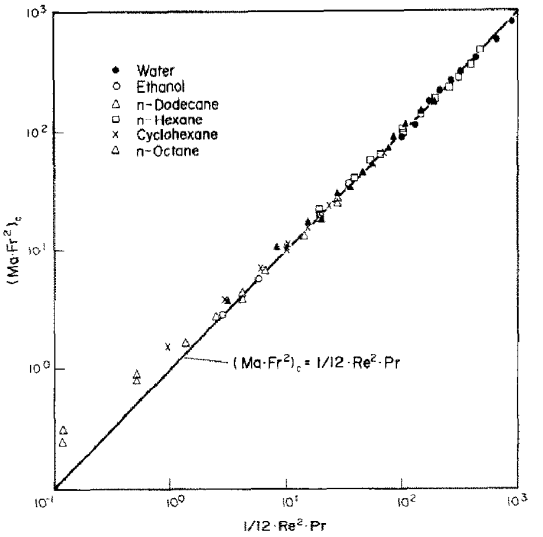

FIG. 11. Comparison of the predicted critical heat flux with experimental data.

successfully both the data of this investigation and those of Ydidsion[16] over a wide range of variables, summarized in Table 2. Deviations occur mainly at very low Reynolds numbers, namely $Re < 5$.

The ability of equation (37) to correlate the critical heat flux data over a wide range of experimental variables and variety of liquids substantiates the validity of the film breakdown criterion as formulated by equation (19). In addition, equation (37) combines the thermocapillary effect, which governs the film rupture, with the critical heat flux in terms of the Marangoni number and relates it to the flow conditions and the liquid physical and thermal properties expressed by the Reynolds, Froude and Prandtl numbers, respectively.

It is worth noting that equation (37) cannot as yet be used for design purposes since m is not known a priori. Consequently, in order to apply it to a specific channel or liquid it is suggested that m be determined by preliminary experiments.

CONCLUSIONS

Isothermal film flow

Surface energy plays an important role in governing the film thickness at the horizontal channel outlet. A realistic downstream boundary condition was formulated, based on minimum specific energy of the film, that successfully predicts this thickness. Axial film thickness profiles can now be predicted within ± 10% for $Re < 150$.

Heated film flow

Thermocapillary forces cause drastic changes in the film thickness relative to isothermal flow. The flow problem that incorporates this effect was solved in conjunction with an experimental surface temperature profile to yield axial film thickness profiles which are in

Table 2. Variables range in critical heat flux runs

Source	Test liquid	Q $(m^2/s) \times 10^6$	$(q/A)_c$ (W/m^2)
This work	Distilled water	5.1–15.5	$(0.98–2.87) \times 10^4$
Ydidsion [16]	Ethanol	0.9–4.0	1080–4080
	n-Hexane	1.3–6.3	420–1730
	n-Octane	0.6–5.2	330–1550
	n-Dodecane	0.2–3.2	380–2080
	Cyclohexane	0.4–4.0	400–1600

reasonable agreement with the measured profiles over the heated section of the channel.

Film breakdown

A mechanism for film rupture and dry patch formation was proposed based on analysis of the effect of surface forces on the film thickness and its stability. It is shown that a dry patch will form first at the downstream edge of the heated section.

Experimental evidence indicates that at the critical heat flux the flow characteristics at the heated section outlet are similar to those of open channel critical flow. Consequently, a simple criterion for film breakdown was formulated stating that rupture occurs when both the film thickness gradient becomes very large and the film attains a critical thickness.

A generalized expression for predicting the critical heat flux was derived based on the critical conditions for film rupture. The equation contains one empirical coefficient and successfully correlates all the available data over a wide range of variables.

REFERENCES

1. W. Leidenfrost, Strömungs- und Wärmeübergangsverhältnisse bei frei Fallenden Rieselfilmen im Zustand der Verdämpfung, *Naturwiss.* **43,** 465–466 (1956).
2. Y. Y. Hsu, F. F. Simon and J. F. Lad, Destruction of a thin liquid film flowing over a heating surface, *Chem. Engng Prog. Symp. Ser.* **61,** 139–152 (1965).
3. F. F. Simon and Y. Y. Hsu, Thermocapillary induced breakdown of a falling liquid film, NASA TN D-5624 (1970).
4. T. Fujita and T. Ueda, Heat transfer to falling liquid films and film breakdown — I. Subcooled liquid films, *Int. J. Heat Mass Transfer* **21,** 97–108 (1978).
5. A. Orell and S. G. Bankoff, Formation of a dry spot in a horizontal liquid film heated from below, *Int. J. Heat Mass Transfer* **14,** 1835–1842 (1971).
6. S. G. Bankoff, Stability of liquid flow down a heated inclined plane, *Int. J. Heat Mass Transfer* **14,** 377–385 (1971).
7. S. P. Lin, Stability of liquid flow down a heated inclined plane, *Letters Heat Mass Transfer* **2,** 361–370 (1975).
8. E. Marschall and C. Y. Lee, Stability of condensate flow down a vertical wall, *Int. J. Heat Mass Transfer* **16,** 41–48 (1973).
9. B. E. Anshus and E. Ruckenstein, The appearance of dry patches on a wetted wall, *J. Coll. Interface Sci.* **51,** 12–22 (1975).
10. N. Zuber and F. W. Staub, Stability of dry patches forming in liquid films flowing over heated surfaces, *Int. J. Heat Mass Transfer* **9,** 897–905 (1966).
11. G. D. McPherson, Axial stability of the dry patch formed in dryout of a two-phase annular flow, *Int. J. Heat Mass Transfer* **13,** 1133–1152 (1970).
12. R. M. Nedderman, The flow of thin films of a viscous liquid down nearly horizontal surfaces, *Chem. Engng Sci.* **21,** 715–717 (1966).
13. A. Gollan and S. Sideman, Single- and two-phase film flow on near horizontal planes, *A. I. Ch. E. Jl* **16,** 1093–1097 (1970).
14. F. Goodridge and G. Gartside, Mass transfer into near-horizontal liquid films, Part I: Hydrodynamic studies, *Trans. Instn Chem. Engrs* **43,** T62–67 (1965).
15. T. Hobler, Laminar flow of a liquid film on a horizontal surface, *Int. Chem. Engng* **12,** 292–294 (1972).
16. Y. Ydidsion, Formation of a dry patch in liquid films flowing over a horizontal heating surface, M.Sc. Thesis, Israel Institute of Technology (1973).
17. V. T. Chow, *Open Channel Hydraulics.* McGraw-Hill, New York (1959).
18. F. M. Henderson, *Open Channel Flow.* MacMillan, Basingstoke (1966).
19. B. Nimmo, Thin film flow on curved surfaces, *Chem. Engng Sci.* **27,** 695–701 (1972).
20. C. S. Yih, Fluid motion induced by surface-tension variation, *Physics Fluids* **11,** 477–480 (1968).
21. A. S. Borodin and J. J. C. Picot, The measurement and prediction of temperatures at the free interface of falling water films under heat transfer, *Can. J. Chem. Engng* **54,** 59–65 (1976).
22. B. Gebhart, *Heat Transfer.* McGraw-Hill, New York (1961).

APPENDIX

We assume that the velocity profile of the heated film is parabolic and is of the form

$$u(x, y) = A(x)y^2 + B(x)y \tag{A1}$$

that satisfies the no-slip condition. Substituting (A1) into the continuity relationship, equation (10), and into the shear stress boundary condition, equation (14), and solving for A and B results in

$$u = \frac{6Q + C_i H^2}{2H^2} y - \frac{6Q + 3C_i H^2}{4H^3} y^2 \tag{A2}$$

where $C_i = (\gamma/\mu)(dT_s/dx)$.

For isothermal film flow $C_i = 0$ and (A2) reduces to

$$u = \frac{3Q}{2H^3}(2Hy - y^2). \tag{A3}$$

This expression was used in Nedderman's analysis [12].

The differential equation for the heated film thickness profile is obtained by integrating the equations of motion with respect to y. Integrating equation (12) between the limits $0 \le y \le H$ subject to the B.C. of equation (15) we obtain

$$P(x, y) = \rho g(H - y) + P_{at} - \sigma \frac{d^2 H}{dx^2}. \tag{A4}$$

Similarly, integrating equation (11) and using the relationship

$$\int_0^H u\frac{\partial u}{\partial x}dy + \int_0^H v\frac{du}{dy}dy = \frac{\partial}{\partial x}\int_0^H u^2\,dy \qquad (A5)$$

there results

$$\frac{\partial}{\partial x}\int_0^H u^2\,dy = -\frac{1}{\rho}\int_0^H \frac{\partial P}{\partial x}dy + \nu\int_0^H \frac{\partial^2 u}{\partial y^2}dy. \qquad (A5)$$

Combining (A5) with (A2) and (A4) and neglecting the effect of film curvature on the axial pressure gradient

$$\frac{\partial}{\partial x}\int_0^H u^2 dy = -\left(\frac{6}{5}\frac{Q^2}{H^2} + \frac{C_i Q}{20} + \frac{C_i^2 H^2}{40}\right)\frac{dH}{dx}$$

$$-\frac{1}{\rho}\int_0^H \frac{\partial P}{\partial x}dy = -gH\frac{dH}{dx}$$

$$\nu\int_0^H \frac{\partial^2 u}{\partial y^2} = -\frac{3Q\nu}{H^2} - \frac{3}{2}C_i\nu.$$

Hence

$$\frac{dH}{dx} = \frac{3Q\nu + \frac{3}{2}C_i\nu H^2}{\frac{6}{5}Q^2 + \frac{C_i Q}{20}H^2 - gH^3 + \frac{C_i^2}{40}H^4}. \qquad (A6)$$

In absence of axial surface temperature gradients (A6) reduces to the case of isothermal film flow, equation (1).

FORMATION D'UNE TRAME ASSECHEE DANS LES FILMS LIQUIDES EN MOUVEMENT DANS UN CANAL HORIZONTAL ET CHAUFFE

Résumé — Les caractéristiques hydrodynamiques et thermiques des films liquides minces s'écoulant dans un canal horizontal et chauffé, sont étudiées expérimentalement et théoriquement pour déterminer l'interruption du film et la formation d'une trame sèche. On formule à partir d'un paramètre empirique et on introduit dans un modèle un critère physique pour l'interruption du film; le flux de chaleur critique est convenablement prédit pour l'eau et des liquides organiques à $5 < Re < 100$. Des équations pour déterminer les profils axiaux d'épaisseur, à la fois pour le film chauffé et non chauffé, sont obtenues à partir d'une condition limite en aval.

DIE BILDUNG VON TROCKENSTELLEN IN STRÖMENDEN FLÜSSIGKEITSFILMEN IN EINEM BEHEIZTEN, HORIZONTALEN KANAL

Zusammenfassung—Die hydrodynamischen und Wärmeübertragungseigenschaften dünner, in einem horizontalen Kanal strömender Flüssigkeitsfilme wurden experimentell und analytisch mit dem Ziel untersucht, den Filmzusammenbruch und die Bildung von Trockenstellen modellhaft zu erfassen. Ein physikalisches Kriterium für den Filmzusammenbruch wurde formuliert und in ein Modell eingefügt, das einen empirischen Parameter enthält und erfolgreich zur Bestimmung der kritischen Wärmestromdichte für Wasser und organische Flüssigkeiten im Bereich $5 < Re < 100$ angewendet werden kann. Gleichungen zur Bestimmung des axialen Filmdicken-Profils für diabate und adiabate Filmströmung wurden unter Benutzung einer stromabwärts vorgeschlagenen Randbedingung abgeleitet.

ОБРАЗОВАНИЕ СУХИХ УЧАСТКОВ НА СТЕНКЕ ПРИ ТЕЧЕНИИ ЖИДКИХ ПЛЕНОК В НАГРЕВАЕМОМ ГОРИЗОНТАЛЬНОМ КАНАЛЕ

Аннотация — Экспериментально и аналитически исследованы гидродинамические и теплообменные характеристики тонких пленок жидкости при течении в горизонтальном нагреваемом канале с целью моделирования разрыва пленки и образования сухих участков. Дан физический критерий разрыва пленки, включаемый в модель, содержащую один эмпирический параметр. В рамках этой модели найдены правильные значения критического теплового потока для воды и органических жидкостей при значениях Re в диапазоне $5 < Re < 100$. Уравнения для расчета аксиальных профилей толщины пленки как при наличии, так и в отсутствие нагрева выведены на основании предложенного граничного условия.